Construction and Building Materials 280 (2021) 122580

Contents lists available at ScienceDirect

Construction and Building Materials

journal homepage: www.elsevier.com/locate/conbuildmat

Valorization of converter steel slag into eco-friendly ultra-high performance concrete by ambient CO_2 pre-treatment

Gang Liu [a,b], Katrin Schollbach [b], Peipeng Li [c,*], H.J.H. Brouwers [b]

[a] School of Human Settlements, Civil Engineering, Xi'an Jiaotong University, Xi'an, China
[b] Department of the Built Environment, Eindhoven University of Technology, P. O. Box 513, 5600MB, Eindhoven, the Netherlands
[c] School of Civil Engineering and Architecture, Wuhan University of Technology, Wuhan 430070, PR China

HIGHLIGHTS

- An ambient CO_2 pre-treatment is conducted to improve the reactivity of steel slag.
- Carbonated steel slag as SCM contributes to a higher strength of UHPC.
- CO_2 can be sequestrated in eco-friendly UHPC by incorporation of carbonated steel slag.
- 45% of cement can be replaced by carbonated steel slag in UHPC (>150 MPa).

ARTICLE INFO

Article history:
Received 19 July 2020
Received in revised form 25 January 2021
Accepted 29 January 2021
Available online 12 February 2021

Keywords:
Converter steel slag
Ultra-high performance concrete
Ambient carbonation
Pozzolanic reaction
Recycling

ABSTRACT

The converter steel slag is a by-product during the steel-making process, which usually acts as an inert ingredient in construction due to the relatively low reactivity. However, its mineral composition results in a high reactivity in a CO_2 rich environment. This study reveals the modification of converter steel slag by an ambient CO_2 pretreatment, and the application of modified converter steel slag as the supplementary cementitious material (SCM) in the design of eco-friendly ultra-high performance concrete (UHPC) by using a particle packing model. The results show that converter steel slag after ambient CO_2 pretreatment is feasible to be used in eco-friendly UHPC design, which achieves a relative higher compressive strength over 150 MPa with the cement substitution from 15% to 45%, compared to non-carbonated steel slag. The ambient CO_2 pretreatment can modify the physical and chemical properties of converter steel slag particles, which produces a rough and porous surface of slag particles because of the precipitation of calcium carbonate and amorphous silica gel as carbonation products. Consequently, the incorporation of carbonated steel slag improves the cement hydration, enhance the formation of ettringite and C-S-H, while densify the microstructure compared to non-carbonated slag in eco-friendly UHPCs. The leaching of potentially hazardous elements, e.g. Cr and V from carbonated steel slag can be efficiently reduced below legal limits in UHPC mixtures.

1. Introduction

Ultra-high performance concrete (UHPC) is a type of concrete which shows a high compressive strength (at least 150 MPa) [1,2] and extremely dense microstructure [3]. As a consequence, excellent durability can be achieved [4–6]. The high mechanical performance can efficiently reduce the volume and mass of the construction. However, in the UHPC design, to reach appropriate workability, a large amount of cement (900–1300 kg/m^3) is usually used [7]. This results in a high cost of UHPC compared to normal concrete [8]. Furthermore, because of the low water-to-binder ratio of UHPC, the hydration degree of cement is limited [9]. Thus, a large quantity of cement remains unreacted and acts as micro-filler. To reduce costs and increase sustainability much attention is paid to industrial by-products, for instance, ground granulated blast furnace slag (GGBFS), fly ash, silica fume and recycled waste glass have been investigated to replace cement in eco-friendly UHPC mixture design [10–13]. The Brouwers mix design method was widely applied to optimize low carbon footprint and eco-friendly UHPC [14–17].

Steel slags are by-products of the steel making process. The EU alone produces about 110 million tons of raw steel, leading to approximately 10 million tons of steel slag annually [18]. In the Netherlands alone 0.7 M tons of converter steel slag are produced annually. Another by-product of steelmaking - ground granulated

* Corresponding author.
E-mail addresses: G.Liu@tue.nl (G. Liu), lipp@whut.edu.cn (P. Li).

https://doi.org/10.1016/j.conbuildmat.2021.122580
0950-0618/

blast furnace slag (GGBFS) has been widely applied as cement replacement because it can be easily activated [19]. In contrast with GGBFS - converter steel slag shows low hydraulic reactivity. It is therefore not widely used in the building industry and mostly limited to aggregates in road construction [20]. The main mineral phases in converter steel slag are larnite, wuestite and brownmillerite. magnetite, and free lime are also found [21–23]. The existence of calcium silicate phases results in the latent hydraulic character of converter steel slag [24]. In recent years, converter steel slag was studied as a supplementary cementitious material (SCM). However, compared to other SCMs that can replace cement in larger amounts, the converter steel slag substitution was limited to around 20% without strength reduction in normal concrete [25,26]. Reports about fine steel slag powder in UHPC are rare, and only a few studies indicate that steel slag addition contributed to a higher flowability. However, a strength reduction still can be observed when steel slag powder beyond 30% is used as cement substitution in UHPC due to the low reactivity [27,28].

It is noteworthy that the converter steel slag, as a calcium silicate rich material, shows a relatively high carbonation reactivity [21–23]. Some studies have therefore attempted to apply steel slags as a CO_2 feedstock material [29]. The CO_2 can be permanently stored as calcium carbonate, which exhibits high thermal stability. Some results showed that the CO_2 uptake ability of steel slag could potentially achieve 200–400 g /kg using a pressurized CO_2 treatment [30]. Some studies focused on the pressurised carbonation treatment for fine or coarse steel slag aggregates, the results indicated that steel slag aggregates can contribute to a better mechanical performance of concrete after carbonation treatment [31]. Additionally, CO_2 can be stored during the carbonation treatment of steel slag. However, the high pressure and temperature used results in significantly increased costs and energy consumption. Recently, some studies indicated that carbonation of fine steel slag powder can take place at ambient conditions and, that the finer steel slag can lead to a higher carbonation reactivity [31–33]. Furthermore, Huijgen et al. have reported CO_2 sequestration capacities of about 100–150 g CO_2/kg with the ground (<38 μm) steel slag powder [34]. These results prove that fine steel slag has the potential to store a large amount of CO_2 with ambient pressure carbonation treatment. Furthermore, ambient carbonation process also provides a possibility to utilize industrial waste gas, which usually contains around 10–20% of CO_2 [35]. On the other hand, the carbonation products of steel slag, such as calcium carbonates and amorphous silica gel can be the reactive mineral ingredients during cement hydration. Thus, the carbonated steel slag powder has the potential to be a new kind of reactive powder as SCM in UHPC design.

In this study, CO_2 is sequestrated in converter steel slag powder by an ambient carbonation pre-treatment. The carbonated and non-carbonated converter steel slag powder is used as cement replacement at different volumes (0–60%) to design a low carbon-footprint eco-friendly UHPC based on a packing model. To clarify the influences of converter steel slag before and after carbonation on the performance of blended UHPC, workability, reaction kinetics, quantification of reaction products, mechanical performance, microstructure and environmental impact are tested and evaluated. The results from this investigation contribute to improving the high-end application and recycling of converter steel slag in eco-friendly and sustainable ultra-high performance concrete manufacture.

2. Materials characterization and test methods

2.1. Materials

The cement used in this study was CEM I 52.5 R, which was produced by ENCI, The Netherlands. The raw converter steel slag (with fractions of 0–5.6 mm) was provided by Tata Steel, IJmuiden, Netherlands. The fine sand (0–0.2 mm) and standard sand (0–2 mm) was used as aggregates in UHPC design, which were provided by Normensand GmbH. The superplasticizer used in this study was polycarboxylic ether based, with a concentration of 35%, provided by Sika. The chemical components of steel slag and cement were identified by using X-ray fluorescence (XRF. PANalytical Epsilon 3) spectroscopy and are shown in Table 1.

2.2. Preparation of CSS powders by ambient carbonation

The steel slag (SS) used in UHPC design was prepared by using a disc mill (Retsch, RS 300 XL). Afterwards, the fine steel slag powder was sprayed with distilled water to reach a solid to water ratio of 0.1. Then the pre-wetted steel slag powder was moved to a climate chamber with a volume of 240 L for ambient pressure carbonation at 25 °C for 72 h. The relative humidity in the chamber was kept at 80%, and circular flow-through CO_2 gas with a concentration of 20% was applied in the chamber continuously. After carbonation for 72 h, no colour was observed after a 0.5% phenolphthalein solution was sprayed on the surface of the carbonated steel slag powder. Finally, the carbonated steel slag (CSS) was dried in the oven at 105 °C for 24 h to remove the free-water, then milled for 5 min to break the agglomeration particles.

2.3. Mix design of UHPC mixtures

In the present study, the reference UHPC mixture was designed based on a packing model using the Brouwers method as shown in:

$$P(D) = \frac{D^q - D^q_{min}}{D^q_{max} - D^q_{min}} \quad (1)$$

$P(D)$ is the cumulative fractions of all particles less than size of D. D_{max} and D_{min} are referred to the maximum particle size and minimum particle size in mixture design. q is the distribution modulus, 0.23 is selected in this research as the recommendations from our previous research due to the high volume of fine powder [3637].

The optimal proportion of each raw material was calculated to achieve an optimum fit between target curve and composed mix according to:

$$RSS = \sum_{i=1}^{n} \left[P_{mix}\left(D_i^{i+1}\right) - P_{tar}\left(D_i^{i+1}\right) \right]^2 \rightarrow min \quad (2)$$

P_{mix} is the designed mix, while P_{tar} is the target grading calculated from Equation (1). The mass of each material in the designed mix are adjusted till an optimum fit between P_{mix} and P_{tar}, an optimization algorithm based on the Least Squares Method (LSM) was conducted during the calculation process.

Table 1
Chemical composition of cement and converter steel slag.

Chemical composition (%)	Converter steel slag	CEM I 52.5 R
CaO	41.55	67.97
SiO_2	11.47	16.19
Al_2O_3	2.24	3.79
Fe_2O_3	31.35	3.59
MgO	3.78	1.71
MnO	4.78	0.09
TiO_2	1.56	0.28
P_2O_5	1.30	0.42
SO_3	0.03	4.05
V_2O_5	1.14	/
Cr_2O_3	0.35	0.01
Cl	0.01	0.04
LOI	0.72	0.51

After the optimal design of the reference mixture, 15%, 30%, 45% and 60% of the cement was replaced by SS or CSS by volume. The water amount of the mixtures was adjusted to achieve a similar flow-ability of 30–33 cm for all mixes. The particle size distributions and recipes of the UHPC mixtures are shown in Fig. 1 and Table. 2.

The mixing of UHPC was conducted using a 5-liter Hobart mixer. Firstly, the dry powders and aggregates were mixed for 30 s at low speed. Then 70% of the total water was added and mixed for another 90 s. After that, the remaining water and superplasticizer were added in the mixer for 120 s at low speed and 120 s at medium speed. Lastly, the fresh UHPC mixtures were filled into the steel moulds of 50 mm × 50 mm × 50 mm and covered with a plastic film for 24 h. After the first 24 h, the UHPC samples were demolded and cured in lime-saturated water until further testing.

2.4. Testing methods

2.4.1. Compressive strength

The compressive strength of UHPC cubes (with a size of 50 mm × 50 mm × 50 mm) was tested after 7 days, 28 days and 91 days curing, which conformed to the EN 12390. An average value was recorded by testing 3 cubes.

2.4.2. Water demand

The water demand of SS and CSS are evaluated by the method of the relative slump, which is conducted according to the previous research [36]. Mixtures with different water to powder ratios were prepared and measured by using a conical mould according to EN 1015–3. Then a trend line can be obtained for analysis.

2.4.3. Calorimetric test

The reaction heat development was measured using an isothermal calorimeter (TAM Air, Thermometric) with the pastes samples without aggregates. The mixtures design of pastes is according to Table 2. The test duration was set to 120 h at a temperature of 20 °C.

2.4.4. XRD and thermal gravimetric tests

A Bruker D8 with a Cu tube was used to determine the hydration products of UHPC mixtures. The crushed pastes samples were immersed in acetone to cease hydration. Then, a ball mill was used to mill the crushed samples into powder for XRD. The Si was used as an internal standard (10%) to conduct the Rietveld quantification for mixtures by using TOPAS V5.

The thermal-gravimetric (TG) analysis was conducted by using a STA 449 F1 instrument. The temperature range was set from 40 °C to 1000 °C, the heating rate was 10 °C/minute and the carrier gas was N_2.

2.4.5. FTIr

The Fourier transform infrared spectroscopy (FTIR) test was performed in a Varian 3100 instrument with the wavenumbers ranging from 4000 to 400 cm^{-1} with a resolution of 4 cm^{-1}.

2.4.6. MIp

The mercury intrusion porosimetry (MIP) was conducted to study the pore size distribution. The UHPC samples after 28 days curing were dried at 105 °C to remove the evaporable water and then crushed into small fractions (4 mm-8 mm) for analysis. The intrusion pressure is from 0 to 227 MPa.

2.4.7. Leaching tests

To evaluate the influence of steel slag and carbonated steel slag UHPC on the environmental impact, a one batch leaching test was performed on the UHPC samples after 28 days curing. The cube was crushed to below 4 mm and leaching test was conducted by using a dynamic shaker, at ambient temperature, and the leaching conditions were L/S (liquid to solid) = 10, 250 rpm and 24 h. The leachates were then filtered through a 0.017–0.030 nm membrane filter. After acidifying the leachates with HNO_3, the concentration of elements in the solutions was measured test by Inductively Coupled Plasma Atomic Emission Spectrometry (ICP-OES) according to one batch leaching test, NEN 6966.

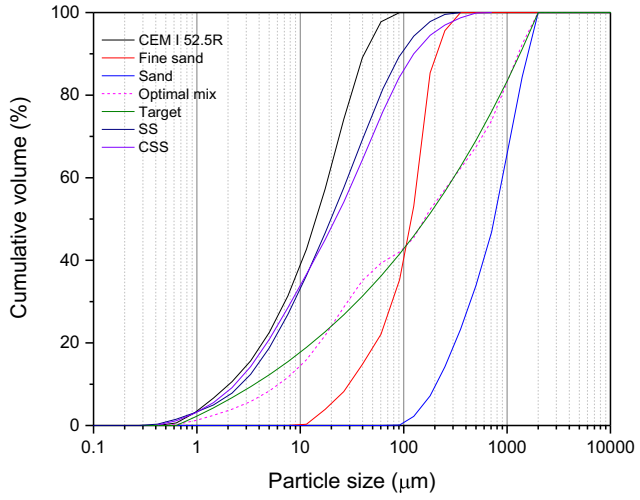

Fig. 1. Particle size distribution of raw materials and optimal UHPC.

3. Results and discussion

3.1. Characterization of converter steel slag after ambient carbonation

3.1.1. Mineral composition

The mineral composition of SS and CSS are shown in Fig. 2. The minerals in SS are related to larnite, magnetite, brownmillerite and wustite, which are typically observed in steel slag [38]. After ambient carbonation treatment, high-intensity calcite peaks can be identified, while a small amount of aragonite is also present in CSS. By using the quantification analysis for SS and CSS, the change of main phases before and after ambient carbonation are shown in Fig. 3. It is clear to see a significant reduction of dicalcium silicate from 29% to 12.8% after carbonation, while brownmillerite content decreases from 13% to 10%. At the same time, the calcium carbonate (including calcite and aragonite) increases from 0.86% to 19% after treatment. The other phases such as wuestite and magnetite exhibit a relatively low reactivity to ambient carbonation. The reaction of dicalcium silicate is also confirmed in FTIR results in Fig. 4. The peak around 878 cm^{-1} is related to the Si-O vibration in dicalcium silicate (larnite) in SS [39]. After carbonation, this signal exhibits a huge reduction, while the location of Si-O shifts to 1070 cm^{-1}. This is induced by the formation of polymerized silica gel after the carbonation reaction of dicalcium silicate phase, which cannot be observed from XRD because of the amorphous structure [40]. At the same time, new peaks at 712 cm^{-1}, 873 cm^{-1} and 1401 cm^{-1} are induced by the presence of C-O in calcium carbonate (calcite and aragonite) [41]. These indicate steel slag powder can be carbonated in the ambient temperature and pressure. The Ca-bearing minerals are the main reactive phases in converter steel slag during carbonation, while calcium carbonate and amorphous silica gel are related to the main reaction products.

Table 2
Mixtures design of UHPC (1 m^3).

Sample	OPC (kg)	SS (kg)	CSS (kg)	Sand 0–0.2 (kg)	Sand 0–2 (kg)	Water (kg)	SP (kg)	Flow ability(mm)
Ref.	925.0	0.0	0.0	287.9	1028.3	177.2	27.8	295
SS15	786.3	160.8	0.0	287.9	1028.3	172.2	27.8	330
SS30	647.5	321.6	0.0	287.9	1028.3	167.2	27.8	315
SS45	508.8	482.4	0.0	287.9	1028.3	162.2	27.8	320
SS60	370.0	643.1	0.0	287.9	1028.3	160.9	27.8	310
CSS15	786.3	0.0	155.5	287.9	1028.3	177.2	27.8	310
CSS30	647.5	0.0	311.0	287.9	1028.3	177.2	27.8	300
CSS45	508.8	0.0	466.5	287.9	1028.3	177.2	27.8	305
CSS60	370.0	0.0	622.0	287.9	1028.3	177.2	27.8	305

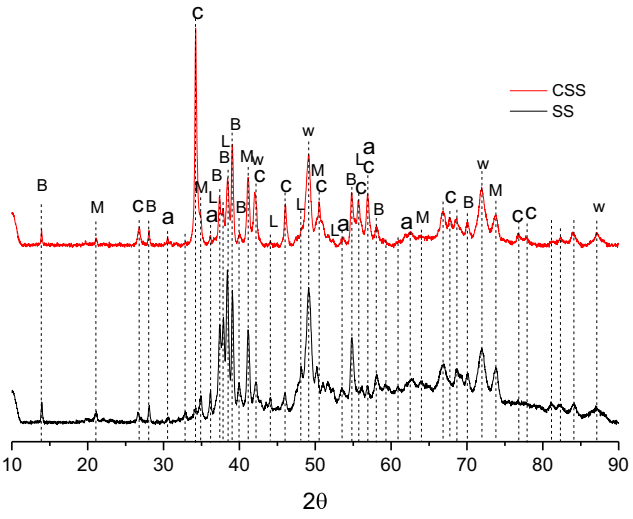

Fig. 2. XRD patterns of converter steel slag after ambient carbonation treatment (B-brownmillerite, M−magnetite, C-calcite, a-aragonite, L-larnite, W-wustite).

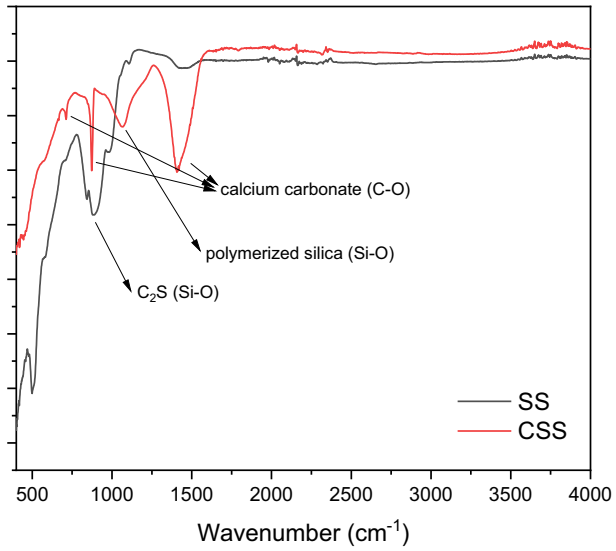

Fig. 4. FTIR of converter steel slag before and after ambient carbonation treatment.

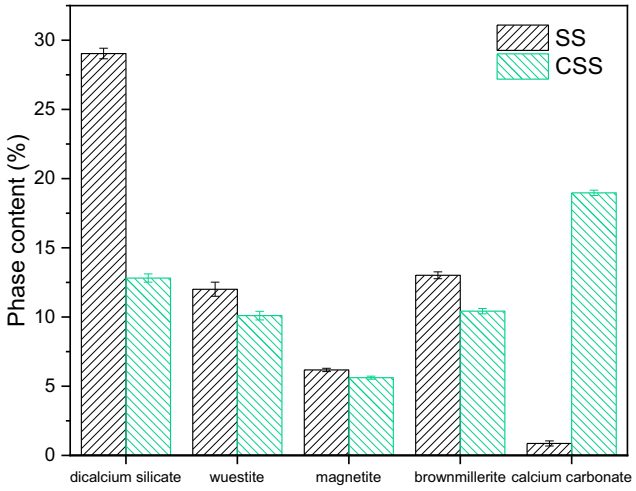

Fig. 3. The variation of main phases in converter steel slag after ambient carbonation treatment.

3.1.2. Physical properties

The physical properties of components, for example, morphology and water demand, effectively affect the workability and performance of designed UHPC. As can be seen in Table 3, the surface area and pore volume of steel slag are increased dramatically after ambient carbonation treatment. This is induced by the reaction of Ca-bearing phases such as C_2S, and the presence of carbonation products. Besides, due to the lower density of calcium carbonate compared to dicalcium silicate [42], the carbonation treatment reduced the specific density of steel slag. Furthermore, the rough and porosity surface of steel slag particles after carbonation also indicates the presence of carbonation products as shown in SEM images (Fig. 5). Generally, such a porous microstructure and high surface area can result in a high water demand, which can influence the performance of UHPC. To clarify this, the results of the water demand of SS and CSS is shown in Fig. 6. Indeed, CSS exhibits a higher water demand compared to SS, which is contributed by the high surface area and porosity. However, in a comparison with our previous research [36], the water demand of CSS is still lower than cement powder even with such a high surface area. This might be due to the presence of the amount of calcium carbonate on the surface of slag particles after ambient carbonation treatment, which can lead to an inter-particle electrostatic repulsion in water [43]. The results in Table 2 (mix design) also confirms a satisfied flowability of CSS blended UHPC mixtures.

3.2. Early hydration of SS/CSS- UHPC

To study the influence of SS and CSS substitution on the hydration of different mixtures, the calorimeter test was conducted and the results are shown in Fig. 7 (a)-(d). For steel slag blended UHPC mixtures, S15 and S30 present a slight enhancement of the intensity of the main peaks to the Ref, which indicates that the addition of 15% of SS could accelerate the early hydration of cement. Meanwhile, a reduction of the main peak intensity and a retardation effect can be observed in S30, S45 and S60. Generally, the hydration intensity and the time of the hydration reaction will

Table 3
Physical properties of materials.

Material	Surface area (m^2/g)	Pore volume (cm^3/g)	Specific density (g/cm^3)	CO_2 uptake (g/kg)	pH
CEM I 52.5R	1.004	0.0089	3.10	/	/
SS	1.153	0.0068	3.90	/	12.3
CSS	21.05	0.0298	3.65	107	10.2

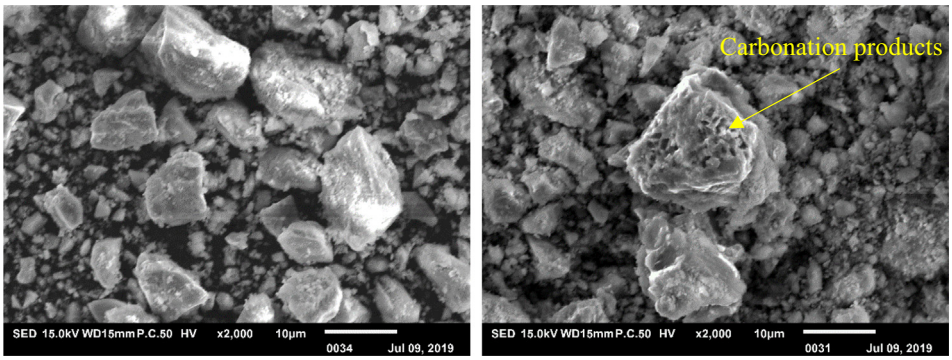

(a) (b)

Fig. 5. SEM images of (a) SS particles, (b) CSS paticles.

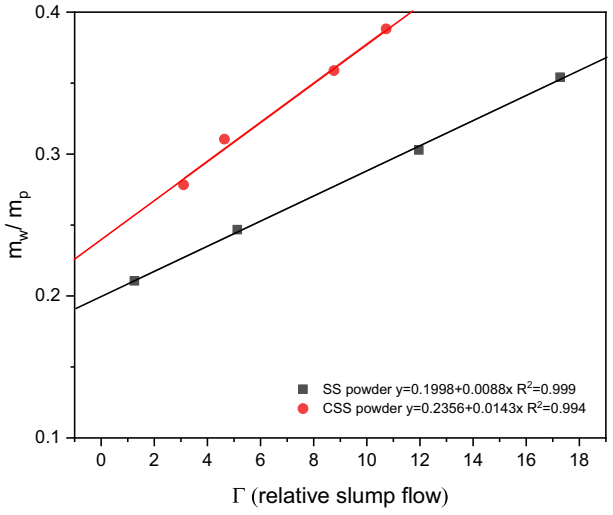

Fig. 6. Water demand of converter steel slag powder before and after ambient carbonation.

be influenced by several factors, such as the change of the effective water-to-cement ratio, superplasticizer to cement ratio, filler effect and nucleation effect [44]. The reduction of the main hydration peak intensity and the increase of time to reach the hydration peak in the blended UHPC mixtures were caused by the higher SP to cement ratio [45,46]. However, the normalized cumulative heat of SS and CSS blended UHPCs are all higher than Ref after the test period and increase with increasing replacement level. This is induced by the filler effect, which increases the effective water-to-cement ratio. As a consequence, cement can achieve a higher reaction degree [47].

As can be seen from the calorimeter results of blended UHPC mixtures, SS blended samples release slightly more cumulative heat than CSS blends with the same replacement ratio. This limited change can be induced by two factors. Firstly, steel slag is well known as a highly alkaline solid by-product, which is due to the leaching of Ca^{2+} [48]. As a consequence, the reaction intensity could be promoted. However, carbonation treatment significantly reduces the larnite content and therefore the Ca^{2+} leaching, as well as the pH [49]. Secondly, the highly porous CSS also absorbs more water which results in a lower effective water amount for hydration, which slightly reduces the total heat compared to SS blends at an early age. It is interesting to notice that the silica gel in CSS shows limited acceleration effect on cement hydration at an early age, this is due to that the amorphous silica gel exists in the inner layer of CSS particles, which is covered by the calcium carbonate [50]. Consequently, the reaction between silica gel and cement is limited in the first days. At high volume replacement ratios (60%), CSS blended UHPC also exhibits a clear shoulder after the main hydration peak, which is not present in SS blended samples. The shoulder is possibly caused by the formation of hemicarboaluminate and the transformation of ettringite [51].

3.3. Performance evaluation of SS/CSS- UHPC

3.3.1. Compressive strength

The compressive strength of UHPC incorporating various volume of SS and CSS after 7, 28 and 91 days curing is shown in Fig. 8. It is observed that all samples present sufficient strength to be classified as UHPC after the test period except SS45, SS60 and CSS60.

At the very early age (7 days), all SS and CSS blended UHPC mixtures exhibit a poor strength performance compared to the reference. Gradual strength reduction occurs with increased replacement ratio for both SS and CSS. The lower mechanical performance of UHPC at early ages is commonly observed if cement is replaced by other low reactivity SCMs or fillers, for example, fly ash and limestone powder [8,27]. However, Ref, SS15, SS30, CSS15 and CSS30 have reached a strength higher than 145 MPa after 28 days of curing. A further increase in strength occurs after 91 days. CSS15, CSS30 and CSS45 exhibit strength of 162 MPa, 159 MPa, and 150 MPa, respectively, while the reference mixture reaches 156 MPa. It should be noted that CSS blended UHPCs show a better strength performance than SS blended UHPCs when cement replacement ratios range from 15% to 45%. When the cement

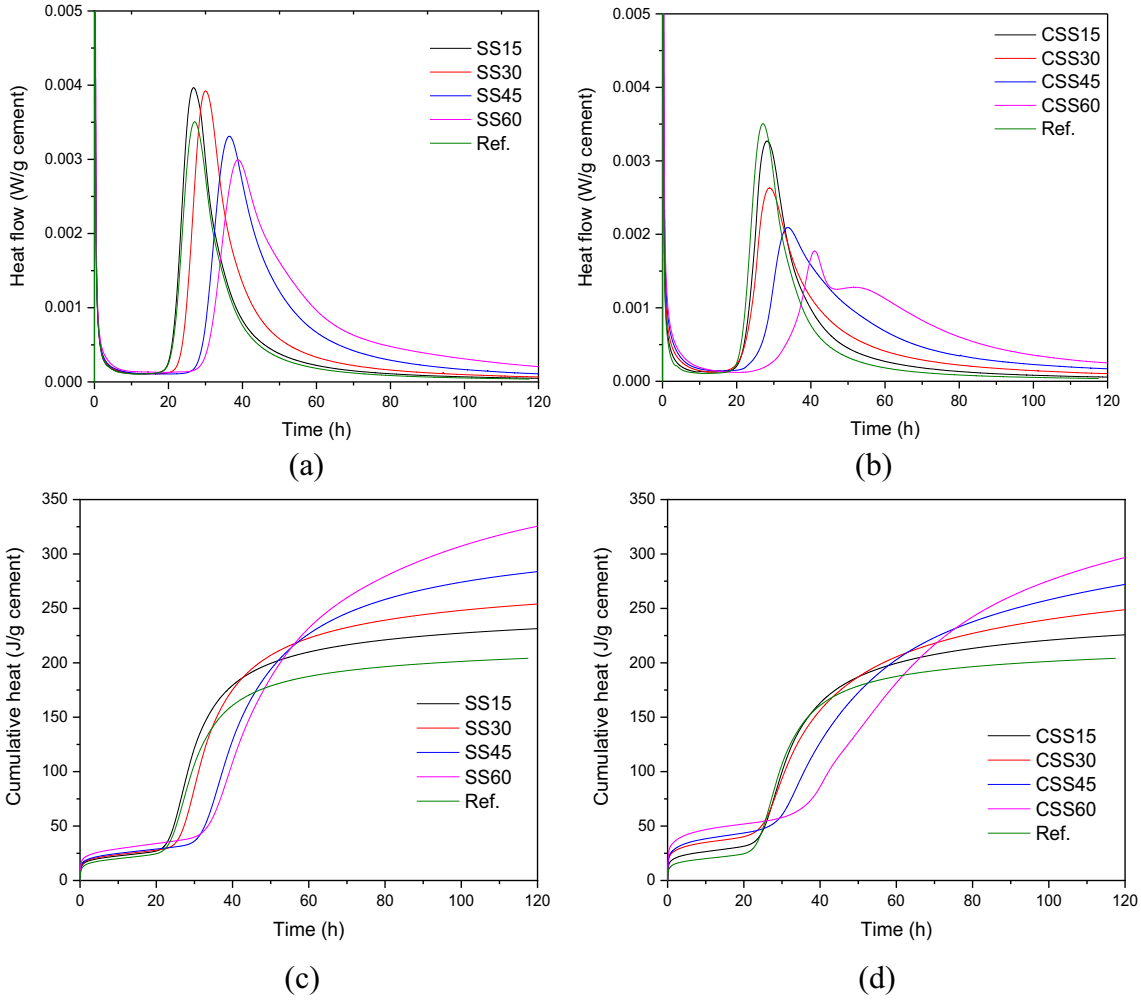

Fig. 7. The heat flow of SS blended binder (a) and CSS blended binder and the cumulative heat of SS blended UHPC binders (c) and CSS blended UHPC binders (d).

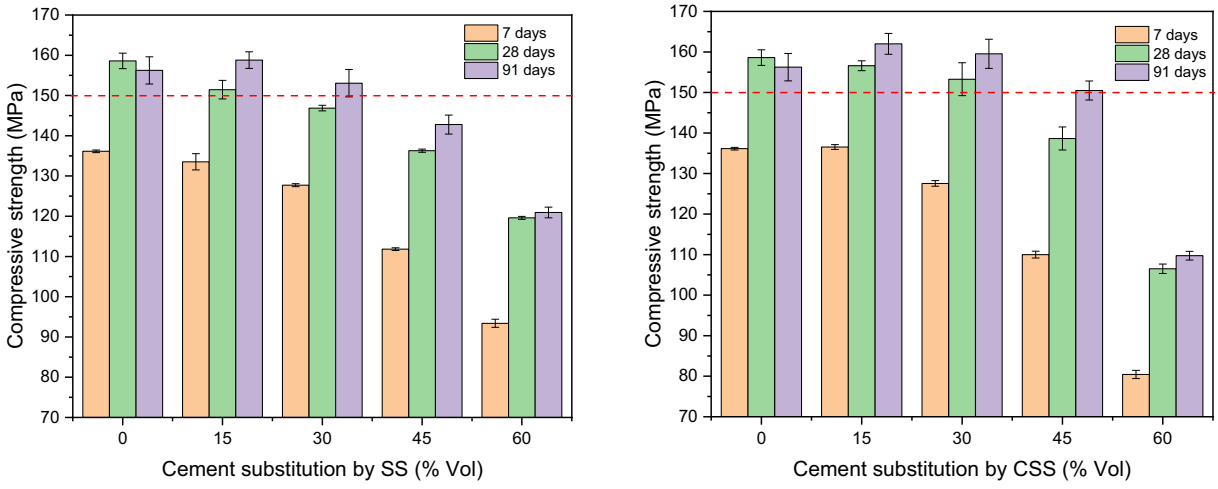

Fig. 8. Compressive strength of UHPC mixtures.

substitution achieves 60%, a significant strength reduction can be observed because of the lack of hydration products [8].

The above strength results imply that ambient carbonation treatment is effective to improve the feasibility of using steel slag in UHPC. Firstly, CSS has a highly porous structure, rough surface and a subsequent high water demand compared to SS as shown in the above results. Therefore, the effective pore water is reduced, as well as the distance between particles, which causes a denser microstructure. Similar observation also can be found in concrete containing carbonated RCA [52] and UHPC containing

manufactured sand [53]. On the other hand, the rough surface also can provide a strengthened bonding between CSS particles and cement pastes. In addition, the water absorbed by CSS particles also can be released gradually at a later age and act as an internal curing agent, which can promote the further hydration of cement, especially in UHPC. Afterwards, further strength development can be observed at later ages. Secondly, the precipitation of carbonation products on the surface of CSS particles also possible to enhance the cement reaction and modify the microstructure of blended UHPC, which will be discussed in the following sections.

3.3.2. Reaction products

3.3.2.1. Quantification of hydration products. The evolution of mineral phases with various cement substitution in the SS and CSS UHPC pastes after 28d hydration is shown in Fig. 9. In the SS samples the amount of magnetite, wuestite, brownmillerite and C_2S increases with the cement substitution ratio, because uncarbonated converter slag is composed of these minerals (Fig. 2). The residual C_3S keeps decreasing at the same time, because the samples contain less cement, while the enhanced effective water to cement ratio also promotes the hydration of cement particles. As a consequence, more C_3S phase reacts at higher substitution levels as can be seen in Fig. 10 (a), where the amount of C_3S is normalized by the overall amount of cement in the sample. Due to the decreasing amount of unreacted C_3S the portlandite content also increases proportionally as shown in Fig. 10 (b). For CSS mixtures, the magnetite, wuestite, brownmillerite and carbonate contents increase with increasing substitution levels, as these are the major phases of carbonated converter slag (Fig. 3). The amount of ettringite is overall higher than in the SS samples. This can be explained by the existence of large amounts of calcium carbonate from CSS in the hydration system, which can promote the formation of ettringite [54]. A similar observation was also reported in the hydration system of OPC-limestone [55]. The second peak in the calorimeter measurement of CSS60 also supports this observation [56].

It is interesting to notice that the unreacted C_3S in SS and CSS UHPC pastes all keep decreasing according to the increase of cement substitution in Fig. 10, which is due to the dilution effect after SS/CSS incorporation. However, the incorporation of CSS in UHPC mixtures results in a lower C_3S content compared to SS. This is likely due to the higher water content in the CSS samples due to the increased water demand of CSS. The porous carbonated slag might even act as internal curing. Then the hydration of the cement part can be improved. In this case, a greater amount of portlandite could have been expected in the CSS samples compared to SS, but this is not the case. Instead, the portlandite content shows a limited increase and even a decrease at the high substitution level, for example, 60% in CSS samples compared to SS as shown in Fig. 10 (b). This indicates that portlandite in CSS samples is consumed in the system and that the consumed amount seems to increase with the substitution level. In Section 3.1, a polymerized silica gel is identified in CSS, which can show a high pozzolanic reactivity [40]. Consequently, when CSS was incorporated in cement based UHPC mixtures, calcium hydroxide from cement hydration can be consumed by the presence of amorphous silica gel. Furthermore, the secondary C-S-H can be formed to fill the void, this also agrees with the results of compressive strength.

3.3.2.2. TG analysis. The thermogravimetric analysis results for the different mixtures is shown in Fig. 11. For all UHPC pastes after 28 days curing, three significant decomposition stages can be observed. The first peak is caused by the part of evaporable water (before 105 °C), decomposition of ettringite (110–170 °C), carboaluminate hydrates and C-S-H (105–400 °C), which overlaps with each other. The following two peaks are resulted by the decomposition of calcium hydroxide and calcium carbonates, respectively

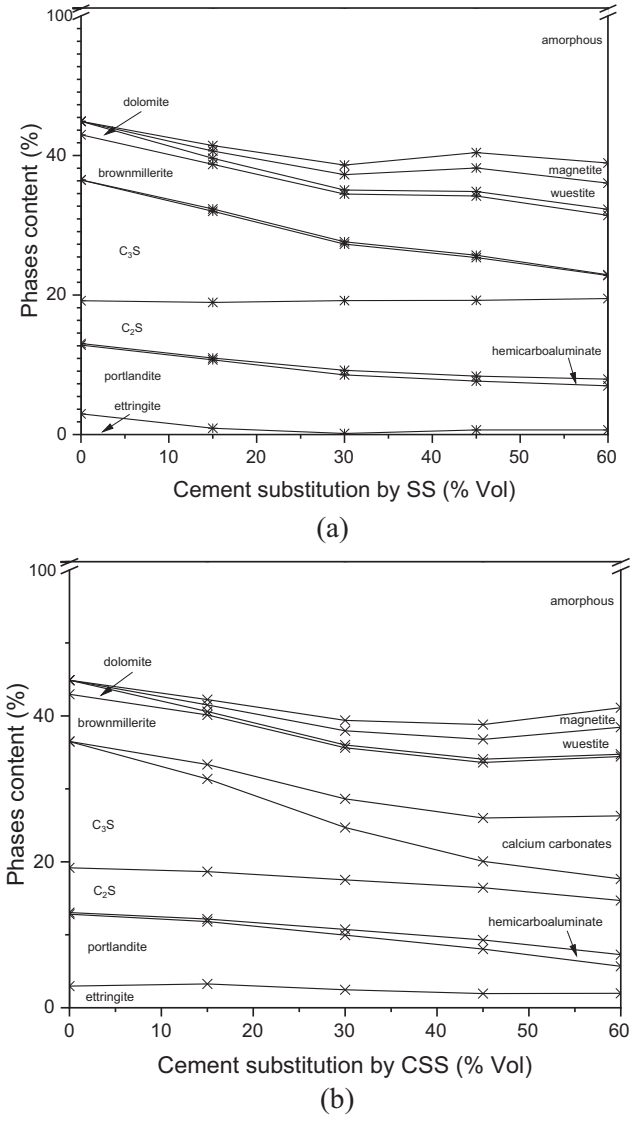

Fig. 9. Quantification of phases in mixtures (a) SS UHPC pastes and (b) CSS UHPC pastes after 28 days curing.

[57,58]. The intensity of peaks is in agreement with the quantification results.

To clarify the influences of SS and CSS on C-S-H formation, the amount of bound water in CSH was plotted normalized by mass of cement (Fig. 12). It is clear that the increase of cement substitution in the SS samples promotes cement hydration, which is reflected by the increase of bound water in C-S-H, as well as the formation of portlandite and consumption of C_3S as discussed in Section 3.3.2.1. The more bound water in C-S-H gel in CSS samples compared to SS is observed. This indicates that CSS mixtures produced more C-S-H by consuming portlandite. The likely reason for this is the fact that the carbonation of C_2S in CSS does not only produce calcite, but also amorphous silica gel [29]. The amorphous silica can exhibits pozzolanic reactivity in OPC based UHPC concrete and increases the formation of secondary C-S-H, which also increases the total amount of water bound in C-S-H [17,59,60] and consumes portlandite.

3.3.2.3. Microstructure. Fig. 13 exhibits the pore size distribution of selected UHPC samples after 28 days. The pore sizes from 5 nm to 300 nm are presented for selected mixtures. The critical pore

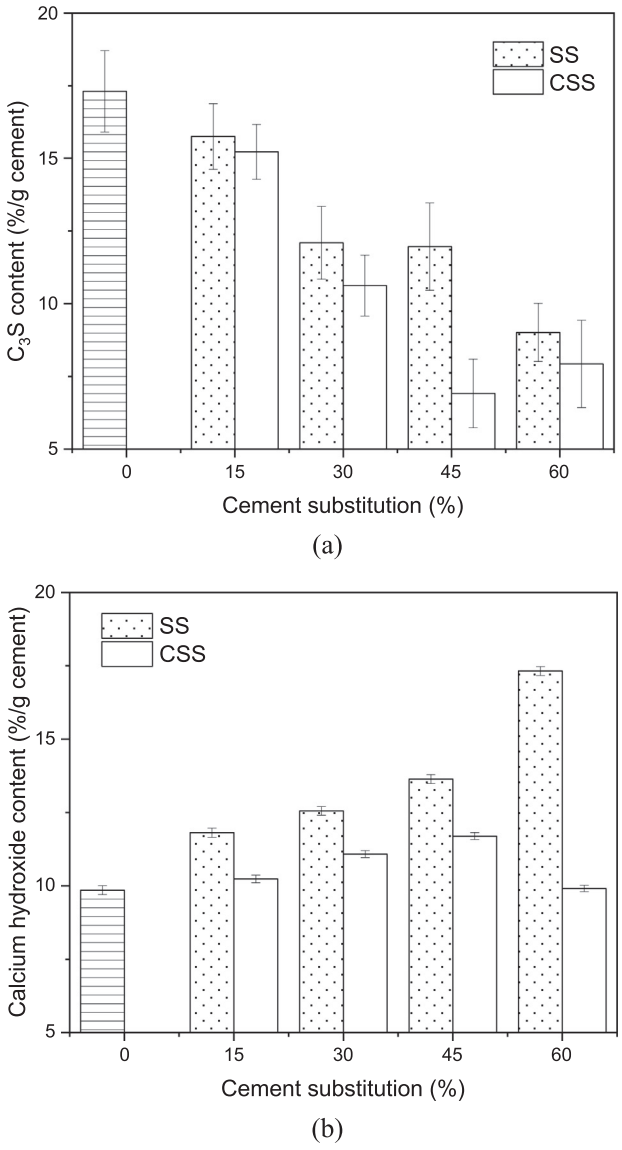

Fig. 10. Normalized content of (a) unreacted C_3S and (b) calcium hydroxide by mass of cement.

diameter (the peak on the pore size curve, defined as the pore size when reaching the highest intrusion rate) of the reference mixture without steel slag occurs at around 40 nm. When 30% steel slag is utilized to replace cement (S30), the peak of the critical pore diameter is higher, because the dilution effect increases the effective water to cement ratio and promotes the formation of porous structures. However, UHPC incorporating 30% carbonated steel slag (CSS30) shows a very similar pore size distribution to the reference only containing cement, which indicates that the dilution effect does not have any negative effect on pore structure, because it will be compensated or overcome by the formation of secondary C-S-H from the pozzolanic reaction of amorphous silica gel [61]. In other words, the steel slag, especially carbonated steel slag could be successfully used to substitute cement in UHPC system. However, too much addition of either steel slag or carbonated steel slag, e.g. 60%, will significantly weaken the microstructure, by greatly shifting the critical pore diameter to larger values (around 50–60 nm), because of the increased reaction products of carbonated steel slag is not enough to fill the pore from additional water compared to SS60, as well as the lack of cement hydration products.

3.4. Leaching property of SS/CSS-UHPC

The leaching results of raw steel slags and UHPC mixtures are shown in Table 4. The leaching of B, Ba, Cr and V are different before and after carbonation of steel slag. B leaching increased from 0.199 mg/L to 0.417 mg/L after carbonation, while Cr and V leaching increased from below the detection limit to 0.047 mg/L and 12.11 mg/L, respectively. On the contrary, the leaching of Ba decreased from 0.236 mg/L to non-detectable. Thus, the carbonation treatment of steel slag dramatically increases Cr and V leaching. C_2S in converter slag contains V and Cr, which reacts during carbonation and decreases the pH overall and causes higher V and Cr leaching [62]. The newly formed carbonates seem not able to incorporate the V and Cr, either.

For the leaching of blended UHPCs, it can be observed that when steel slag and carbonated steel slag are used as a cement replacement, Ba, Cr and V leaching are significantly reduced to below the legislative limit of the Dutch SQD (Soil Quality Decree). Generally, ordinary Portland cement can be used to stabilize harmful ions in practical constructions. As reported in a previous study of cement based materials, the Cr and V can be absorbed in cement hydration products, for example, AFt and AFm phases [63]. The high pH in the concrete pore solution also keeps Cr and V in a less

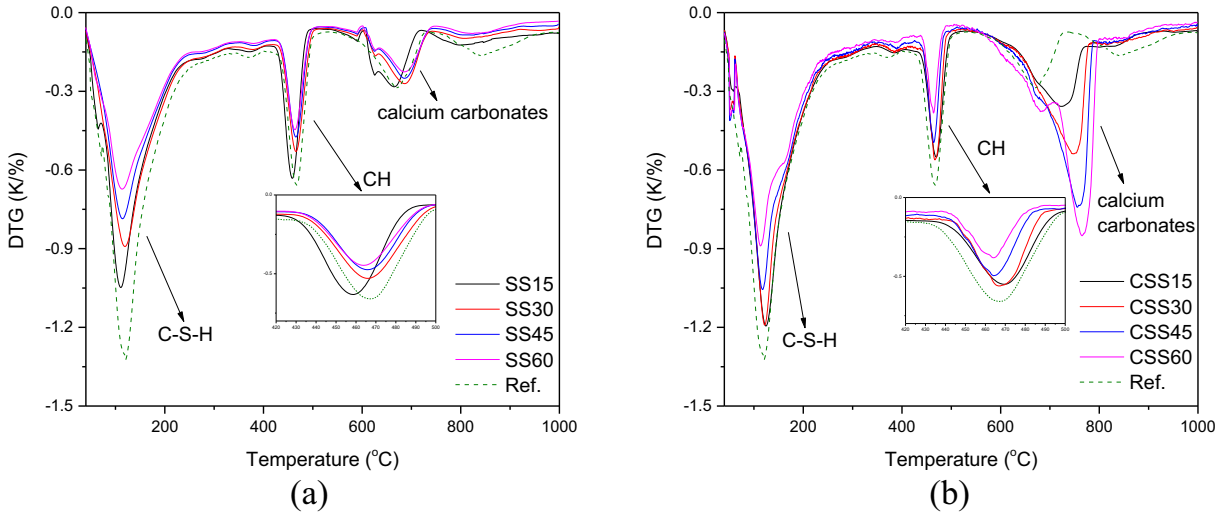

Fig. 11. TG results of UHPC mixtures (a) SS blended samples, (b) CSS blended samples after 28 days.

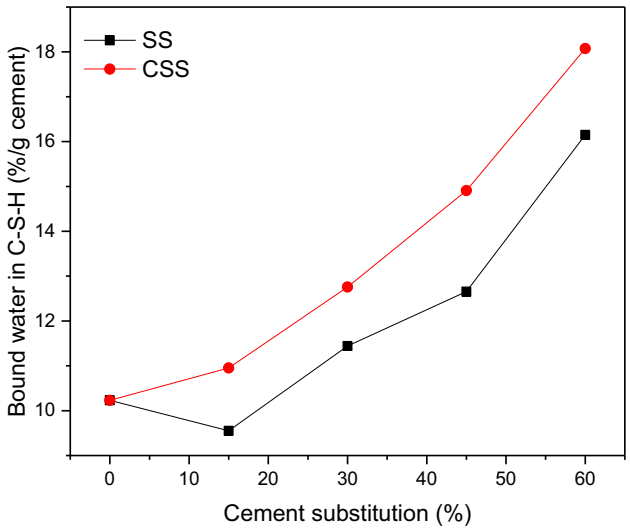

Fig. 12. Bound water in C-S-H as determined by TG between 105 °C and 400 °C.

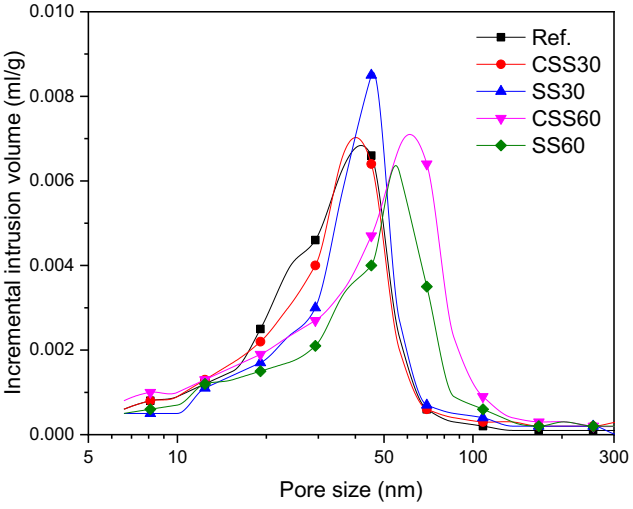

Fig. 13. Pore size distribution of blended UHPC.

soluble state [64,65]. However, the concentration of Ba was increased for steel slag and carbonated steel slag blended UHPC mixtures, which is higher than that of the raw materials. This indicates that the Ba leaching is mostly contributed by the cement [66]. This observation agrees with the previous investigation that application of carbonated steel slag as aggregates in concrete [67].

4. Conclusions

The present study investigates the effect of ambient CO_2 pretreatment of converter steel slag on the valorization of converter steel slag as a supplementary cementitious material in eco-friendly UHPC design. Converter steel slag after an ambient carbonation pretreatment is more feasible to be cement substitution in blended UHPC than before. The properties of converter steel slag after ambient carbonation are characterized. Then the workability, hydration kinetics, hydration products, microstructure and environmental impact of sustainable UHPCs are evaluated. The main conclusions are as follows:

1. The dicalcium silicate (C_2S) and browmillerite in SS powder are observed to show reactivity during ambient carbonation. The CO_2 uptake achieves 107 g/kg steel slag. The consequent carbonation products – calcium carbonate and amorphous silica gel are identified by using XRD and FTIR, respectively. The rough and porous surface of CSS is presented in SEM image, which is due to the presence of calcium carbonate and silica gel as carbonation products. Therefore, CSS powder exhibits a slightly higher water demand than SS powder due to the porous surface after carbonation. However, CSS and SS blended UHPC samples still have a better flowability than that of the reference OPC sample.
2. The UHPCs incorporating CSS present a higher compressive strength than SS samples when the replacement ratio is below 60%. When the cement was substituted by 15% –45% CSS, compressive strengths between 150 MPa and 162 MPa can be obtained. For SS samples, only 15% – 30% of steel slag can be applied, which present a compressive strength between 150 MPa and 158 MPa.
3. The quantification results of reaction products indicate that CSS powder addition can improve the cement clinker hydration, such as C_3S compared to SS powder. At the same time, the reduction of calcium hydroxide content in CSS samples is observed, which is due to the presence of ambient carbonation product- amorphous silica gel. The enhanced bound water in hydration products in CSS samples also confirms the formation of secondary C-S-H by the pozzolanic reaction of silica gel.
4. The pore size distribution indicates that CSS contributes to a denser microstructure and a smaller critical pore size than SS in UHPCs due to the additional C-S-H formation. However, high replacement ratios, e.g. 60% exhibit a negative effect on the microstructure development by increasing the critical pore size, which is due to the lack of hydration products.
5. The ambient carbonation treatment of SS powder results in high leaching of V and Cr of CSS due to the decomposition of C_2S phase. However, the hydration products and dense structure

Table 4
Leaching of raw materials and UHPC samples.

	B (mg/L)	Ba (mg/L)	Cr (mg/L)	V (mg/L)
Limit in SQD	N.A.	2.2	0.063	0.18
Carbonated steel slag	0.417 (0.002)	L.D.	0.047 (0.002)	12.11 (0.013)
Steel slag	0.199 (0.001)	0.236 (0.010)	L.D.	0.005 (0.001)
OPC	L.D.	0.585 (0.001)	0.016 (0.001)	L.D.
S15	L.D.	0.668 (0.012)	0.006 (0.001)	L.D.
S30	L.D.	0.549 (0.001)	0.004 (0.001)	L.D.
S45	L.D.	0.515 (0.007)	0.002 (0.001)	L.D.
S60	L.D.	0.523 (0.005)	0.001 (0.001)	L.D.
CS15	L.D.	0.532 (0.001)	0.008 (0.001)	L.D.
CS30	L.D.	0.413 (0.001)	0.005 (0.001)	L.D.
CS45	L.D.	0.419 (0.002)	0.004 (0.001)	L.D.
CS60	L.D.	0.290 (0.010)	0.003 (0.001)	L.D.

L.D. – lower than the detection limit. SQD – Soil quality decree in the Netherlands (L/S = 10).

of UHPC can effectively solidify V and Cr, therefore, the leaching results of CSS blended UHPC satisfies the requirement of Soil Quality Decree (SQD) in the Netherlands.

CRediT authorship contribution statement

Gang Liu: Conceptualization, Methodology, Validation, Writing - original draft. **Katrin Schollbach:** Writing - review & editing. **Peipeng Li:** Conceptualization. **H.J.H. Brouwers:** Writing - review & editing, Supervision.

Declaration of Competing Interest

The authors declare that they have no known competing financial interests or personal relationships that could have appeared to influence the work reported in this paper.

Acknowledgements

This research was supported by the funding of China Scholarship Council (No. 201606300062) and Eindhoven University of Technology. Furthermore, the authors wish to express their gratitude to Tata Steel, IJmuiden, Netherlands for the supporting of raw materials and XRD.

References

[1] K. Habel, M. Viviani, E. Denarié, E. Brühwiler, Development of the mechanical properties of an Ultra-High Performance Fiber Reinforced Concrete (UHPFRC), Cem. Concr. Res. 36 (7) (Jul. 2006) 1362–1370, https://doi.org/10.1016/j.cemconres.2006.03.009.
[2] K. Wille, A.E. Naaman, G.J. Parra-Montesinos, Ultra-high performance Concrete with compressive strength exceeding 150 MPa (22 ksi): A simpler way, ACI Mater. J. 108 (1) (Jan. 2011) 46–54, https://doi.org/10.14359/51664215.
[3] M. Verma, P.R. Prem, J. Rajasankar, B.H. Bharatkumar, On low-energy impact response of ultra-high performance concrete (UHPC) panels, Mater. Des. 92 (Feb. 2016) 853–865, https://doi.org/10.1016/j.matdes.2015.12.065.
[4] F. de Larrard, T. Sedran, Optimization of ultra-high-performance concrete by the use of a packing model, Cem. Concr. Res. 24 (6) (1994) 997–1009, https://doi.org/10.1016/0008-8846(94)90022-1.
[5] P.P. Li, H.J.H. Brouwers, W. Chen, Q. Yu, Optimization and characterization of high-volume limestone powder in sustainable ultra-high performance concrete, Constr. Build. Mater. 242 (2020) 118112, https://doi.org/10.1016/j.conbuildmat.2020.118112.
[6] P.P. Li, H.J.H. Brouwers, Q. Yu, Influence of key design parameters of ultra-high performance fibre reinforced concrete on in-service bullet resistance, Int. J. Impact Eng. 136 (2020) 103434, https://doi.org/10.1016/j.ijimpeng.2019.103434.
[7] P. Rossi, Influence of fibre geometry and matrix maturity on the mechanical performance of ultra high-performance cement-based composites, Cem. Concr. Compos. 37 (1) (Mar. 2013) 246–248, https://doi.org/10.1016/j.cemconcomp.2012.08.005.
[8] W. Huang, H. Kazemi-Kamyab, W. Sun, K. Scrivener, Effect of cement substitution by limestone on the hydration and microstructural development of ultra-high performance concrete (UHPC), Cem. Concr. Compos. 77 (Mar. 2017) 86–101, https://doi.org/10.1016/J.CEMCONCOMP.2016.12.009.
[9] A. Korpa, T. Kowald, R. Trettin, Phase development in normal and ultra high performance cementitious systems by quantitative X-ray analysis and thermoanalytical methods, Cem. Concr. Res. 39 (2) (Feb. 2009) 69–76, https://doi.org/10.1016/j.cemconres.2008.11.003.
[10] E. Ghafari, S.A. Ghahari, H. Costa, E. Júlio, A. Portugal, L. Durães, Effect of supplementary cementitious materials on autogenous shrinkage of ultra-high performance concrete, Constr. Build. Mater. 127 (2016) 43–48, https://doi.org/10.1016/j.conbuildmat.2016.09.123.
[11] H. Kim, T. Koh, S. Pyo, Enhancing flowability and sustainability of ultra high performance concrete incorporating high replacement levels of industrial slags, Constr. Build. Mater. 123 (2016) 153–160, https://doi.org/10.1016/j.conbuildmat.2016.06.134.
[12] P.S. Ambily, C. Umarani, K. Ravisankar, P.R. Prem, B.H. Bharatkumar, N.R. Iyer, Studies on ultra high performance concrete incorporating copper slag as fine aggregate, Constr. Build. Mater. 77 (2015) 233–240, https://doi.org/10.1016/j.conbuildmat.2014.12.092.
[13] T. Chen, X. Gao, M. Ren, Effects of autoclave curing and fly ash on mechanical properties of ultra-high performance concrete, Constr. Build. Mater. 158 (2018) 864–872, https://doi.org/10.1016/j.conbuildmat.2017.10.074.
[14] P.P. Li, Q.L. Yu, H.J.H. Brouwers, Effect of PCE-type superplasticizer on early-age behaviour of ultra-high performance concrete (UHPC), Constr. Build. Mater. 153 (Oct. 2017) 740–750, https://doi.org/10.1016/j.conbuildmat.2017.07.145.
[15] H. J. H. Brouwers, "Particle-size distribution and packing fraction of geometric random packings," Phys. Rev. E - Stat. Nonlinear, Soft Matter Phys., vol. 74, no. 3, 2006, doi: 10.1103/PhysRevE.74.031309.
[16] H.J.H. Brouwers, H.J. Radix, Self-compacting concrete: Theoretical and experimental study, Cem. Concr. Res. 35 (11) (2005) 2116–2136, https://doi.org/10.1016/j.cemconres.2005.06.002.
[17] P.P. Li, Y.Y.Y. Cao, H.J.H. Brouwers, W. Chen, Q.L. Yu, Development and properties evaluation of sustainable ultra-high performance pastes with quaternary blends, J. Clean. Prod. 240 (2019) 118124, https://doi.org/10.1016/j.jclepro.2019.118124.
[18] EUROFER, "European Steel in Figures 2018," 2018.
[19] J. Escalante, L. Gómez, K. Johal, G. Mendoza, H. Mancha, J. Méndez, Reactivity of blast-furnace slag in Portland cement blends hydrated under different conditions, Cem. Concr. Res. 31 (10) (Oct. 2001) 1403–1409, https://doi.org/10.1016/S0008-8846(01)00587-7.
[20] W. Qiang, S. Mengxiao, Y. Jun, Influence of classified steel slag with particle sizes smaller than 20 μm on the properties of cement and concrete, Constr. Build. Mater. 123 (Oct. 2016) 601–610, https://doi.org/10.1016/J.CONBUILDMAT.2016.07.042.
[21] M.H. El-Naas, M. El Gamal, S. Hameedi, A.M.O. Mohamed, CO2 sequestration using accelerated gas-solid carbonation of pre-treated EAF steel-making bag house dust, J. Environ. Manage. 156 (2015) 218–224, https://doi.org/10.1016/j.jenvman.2015.03.040.
[22] R. Baciocchi, G. Costa, A. Polettini, R. Pomi, Effects of thin-film accelerated carbonation on steel slag leaching, J. Hazard. Mater. 286 (Apr. 2015) 369–378, https://doi.org/10.1016/J.JHAZMAT.2014.12.059.
[23] K.R. Reddy, J.K. Chetri, G. Kumar, D.G. Grubb, Effect of basic oxygen furnace slag type on carbon dioxide sequestration from landfill gas emissions, Waste Manag. 85 (Feb. 2019) 425–436, https://doi.org/10.1016/J.WASMAN.2019.01.013.
[24] Q. Wang, P. Yan, Hydration properties of basic oxygen furnace steel slag, Constr. Build. Mater. 24 (7) (Jul. 2010) 1134–1140, https://doi.org/10.1016/J.CONBUILDMAT.2009.12.028.
[25] S. Kourounis, S. Tsivilis, P.E. Tsakiridis, G.D. Papadimitriou, Z. Tsibouki, Properties and hydration of blended cements with steelmaking slag, Cem. Concr. Res. 37 (6) (Jun. 2007) 815–822, https://doi.org/10.1016/J.CEMCONRES.2007.03.008.
[26] S. Yang, J. Wang, S. Cui, H. Liu, X. Wang, Impact of four kinds of alkanolamines on hydration of steel slag-blended cementitious materials, Constr. Build. Mater. 131 (Jan. 2017) 655–666, https://doi.org/10.1016/J.CONBUILDMAT.2016.09.060.
[27] X. Zhang, S. Zhao, Z. Liu, F. Wang, Utilization of steel slag in ultra-high performance concrete with enhanced eco-friendliness, Constr. Build. Mater. 214 (Jul. 2019) 28–36, https://doi.org/10.1016/j.conbuildmat.2019.04.106.
[28] J. Liu, R. Guo, Applications of Steel Slag Powder and Steel Slag Aggregate in Ultra-High Performance Concrete, Adv. Civ. Eng. 2018 (2018) 1–8, https://doi.org/10.1155/2018/1426037.
[29] W.J.J. Huijgen, R.N.J. Comans, Carbonation of steel slag for CO2 sequestration: Leaching of products and reaction mechanisms, Environ. Sci. Technol. 40 (8) (2006) 2790–2796, https://doi.org/10.1021/es052534b.
[30] P.S. Humbert, J. Castro-Gomes, CO2 activated steel slag-based materials: A review, J. Clean. Prod. 208 (Jan. 2019) 448–457, https://doi.org/10.1016/J.JCLEPRO.2018.10.058.
[31] B. Pang, Z. Zhou, X. Cheng, P. Du, H. Xu, ITZ properties of concrete with carbonated steel slag aggregate in salty freeze-thaw environment, Constr. Build. Mater. 114 (Jul. 2016) 162–171, https://doi.org/10.1016/J.CONBUILDMAT.2016.03.168.
[32] G. Abdul-baki, Development of vacuum carbonation curing technology for concrete at ambient conditions, McGill University (2017).
[33] B. Pang, Z. Zhou, P. Hou, P. Du, L. Zhang, H. Xu, Autogenous and engineered healing mechanisms of carbonated steel slag aggregate in concrete, Constr. Build. Mater. 107 (Mar. 2016) 191–202, https://doi.org/10.1016/J.CONBUILDMAT.2015.12.191.
[34] W.J.J. Huijgen, R.N.J. Comans, Mineral CO 2 Sequestration by Steel Slag Carbonation, Environ. Sci. Technol. 39 (24) (2005) 9676–9682, https://doi.org/10.1021/es050795f10.1021/es050795f.s001.
[35] I. Taniguchi, T. Yamada, Low Energy CO2 Capture by Electrodialysis, Energy Procedia 114 (2017) 1615–1620, https://doi.org/10.1016/j.egypro.2017.03.1902.
[36] P.P. Li, Q.L. Yu, H.J.H. Brouwers, Effect of coarse basalt aggregates on the properties of Ultra-high Performance Concrete (UHPC), Constr. Build. Mater. 170 (May 2018) 649–659, https://doi.org/10.1016/j.conbuildmat.2018.03.109.
[37] R. Yu, P. Spiesz, H.J.H. Brouwers, Development of Ultra-High Performance Fibre Reinforced Concrete (UHPFRC): Towards an efficient utilization of binders and fibres, Constr. Build. Mater. 79 (Mar. 2015) 273–282, https://doi.org/10.1016/j.conbuildmat.2015.01.050.
[38] R. Baciocchi, G. Costa, M. Di Gianfilippo, A. Polettini, R. Pomi, A. Stramazzo, Thin-film versus slurry-phase carbonation of steel slag: CO2 uptake and effects on mineralogy, J. Hazard. Mater. 283 (Feb. 2015) 302–313, https://doi.org/10.1016/J.JHAZMAT.2014.09.016.

[39] W. Ashraf, J. Olek, "Carbonation behavior of hydraulic and non-hydraulic calcium silicates: potential of utilizing low-lime calcium silicates in cement-based materials," doi: 10.1007/s10853-016-9909-4.
[40] M. Zajac, J. Skocek, P. Durdzinski, F. Bullerjahn, J. Skibsted, and M. Ben Haha, "Effect of carbonated cement paste on composite cement hydration and performance," Cem. Concr. Res., vol. 134, p. 106090, Aug. 2020, doi: 10.1016/j.cemconres.2020.106090.
[41] T. Siva, S. Muralidharan, S. Sathiyanarayanan, E. Manikandan, M. Jayachandran, Enhanced Polymer Induced Precipitation of Polymorphous in Calcium Carbonate: Calcite Aragonite Vaterite Phases, J. Inorg. Organomet. Polym. Mater. 27 (3) (2017) 770–778, https://doi.org/10.1007/s10904-017-0520-1.
[42] S. Liu, X. Guan, H. Zhang, Y. Wang, M. Gou, Revealing the Microstructure Evolution and Carbonation Hardening Mechanism of β-C2S Pastes by Backscattered Electron Images, Materials (Basel) 12 (9) (May 2019) 1561, https://doi.org/10.3390/ma12091561.
[43] D.P. Bentz, C.F. Ferraris, S.Z. Jones, D. Lootens, F. Zunino, Limestone and silica powder replacements for cement: Early-age performance, Cem. Concr. Compos. 78 (Apr. 2017) 43–56, https://doi.org/10.1016/j.cemconcomp.2017.01.001.
[44] P. Lawrence, M. Cyr, E. Ringot, Mineral admixtures in mortars: Effect of inert materials on short-term hydration, Cem. Concr. Res. 33 (12) (Dec. 2003) 1939–1947, https://doi.org/10.1016/S0008-8846(03)00183-2.
[45] K. Yamada, T. Takahashi, S. Hanehara, M. Matsuhisa, Effects of the chemical structure on the properties of polycarboxylate-type superplasticizer, Cem. Concr. Res. 30 (2) (2000) 197–207, https://doi.org/10.1016/S0008-8846(99)00230-6.
[46] Y. Zhang, X. Kong, Correlations of the dispersing capability of NSF and PCE types of superplasticizer and their impacts on cement hydration with the adsorption in fresh cement pastes, Cem. Concr. Res. 69 (2015) 1–9, https://doi.org/10.1016/j.cemconres.2014.11.009.
[47] C. Shi, Z. Wu, J. Xiao, D. Wang, Z. Huang, Z. Fang, A review on ultra high performance concrete: Part I. Raw materials and mixture design, Constr. Build. Mater. 101 (Dec. 2015) 741–751, https://doi.org/10.1016/J.CONBUILDMAT.2015.10.088.
[48] H. I. Gomes, W. M. Mayes, M. Rogerson, D. I. Stewart, I. T. Burked, "Alkaline residues and the environment: A review of impacts, management practices and opportunities," J. Clean. Product., vol. 112. Elsevier Ltd, pp. 3571–3582, 2016, doi: 10.1016/j.jclepro.2015.09.111.
[49] J. Chang, D. Wang, Y. Fang, Effects of mineralogical changes in BOFS during carbonation on pH and Ca and Si leaching, Constr. Build. Mater. 192 (Dec. 2018) 584–592, https://doi.org/10.1016/j.conbuildmat.2018.10.057.
[50] P. Librandi, P. Nielsen, G. Costa, R. Snellings, M. Quaghebeur, R. Baciocchi, "Mechanical and environmental properties of carbonated steel slag compacts as a function of mineralogy and CO2 uptake," J. CO2 Util., vol. 33, pp. 201–214, Oct. 2019, doi: 10.1016/j.jcou.2019.05.028.
[51] D. Wang, C. Shi, N. Farzadnia, Z. Shi, H. Jia, Z. Ou, A review on use of limestone powder in cement-based materials: Mechanism, hydration and microstructures, Constr. Build. Mater. 181 (Aug. 2018) 659–672, https://doi.org/10.1016/J.CONBUILDMAT.2018.06.075.
[52] D. Xuan, B. Zhan, C.S. Poon, Assessment of mechanical properties of concrete incorporating carbonated recycled concrete aggregates, Cem. Concr. Compos. 65 (Jan. 2016) 67–74, https://doi.org/10.1016/j.cemconcomp.2015.10.018.
[53] R. Yang, R. Yu, Z. Shui, C. Guo, S. Wu, X.u. Gao, S. Peng, The physical and chemical impact of manufactured sand as a partial replacement material in Ultra-High Performance Concrete (UHPC), Cem. Concr. Compos. 99 (2019) 203–213, https://doi.org/10.1016/j.cemconcomp.2019.03.020.
[54] B. Lothenbach, G. Le Saout, E. Gallucci, K. Scrivener, Influence of limestone on the hydration of Portland cements, Cem. Concr. Res. 38 (6) (Jun. 2008) 848–860, https://doi.org/10.1016/j.cemconres.2008.01.002.
[55] G. Kakali, S. Tsivilis, E. Aggeli, M. Bati, Hydration products of C3A, C3S and Portland cement in the presence of CaCO3, Cem. Concr. Res. 30 (7) (2000) 1073–1077, https://doi.org/10.1016/S0008-8846(00)00292-1.
[56] D. Wang, C. Shi, N. Farzadnia, Z. Shi, H. Jia, Z. Ou, "A review on use of limestone powder in cement-based materials: Mechanism, hydration and microstructures," Construct. Build. Mater., vol. 181. Elsevier Ltd, pp. 659–672, 30-Aug-2018, doi: 10.1016/j.conbuildmat.2018.06.075.
[57] L. Alarcon-Ruiz, G. Platret, E. Massieu, A. Ehrlacher, The use of thermal analysis in assessing the effect of temperature on a cement paste, Cem. Concr. Res. 35 (3) (Mar. 2005) 609–613, https://doi.org/10.1016/j.cemconres.2004.06.015.
[58] E. T. Stepkowska, J. M. Blanes, F. Franco, C. Real, J. L. Pérez-Rodríguez, "Phase transformation on heating of an aged cement paste," in Thermochimica Acta, 2004, vol. 420, no. 1-2 SPEC. ISS., pp. 79–87, doi: 10.1016/j.tca.2003.11.057.
[59] R. Yu, P. Spiesz, H.J.H. Brouwers, Effect of nano-silica on the hydration and microstructure development of Ultra-High Performance Concrete (UHPC) with a low binder amount, Constr. Build. Mater. 65 (Aug. 2014) 140–150, https://doi.org/10.1016/j.conbuildmat.2014.04.063.
[60] A. Schöler, B. Lothenbach, F. Winnefeld, M. Zajac, Hydration of quaternary Portland cement blends containing blast-furnace slag, siliceous fly ash and limestone powder, Cem. Concr. Compos. 55 (2015) 374–382, https://doi.org/10.1016/j.cemconcomp.2014.10.001.
[61] P.P. Li, Q.L. Yu, H.J.H. Brouwers, W. Chen, Conceptual design and performance evaluation of two-stage ultra-low binder ultra-high performance concrete, Cem. Concr. Res. 125 (2019) 105858, https://doi.org/10.1016/j.cemconres.2019.105858.
[62] C. van Hoek, J. Small, S. van der Laan, Large-Area Phase Mapping Using PhAse Recognition and Characterization (PARC) Software, Micros. Today 24 (5) (Sep. 2016) 12–21, https://doi.org/10.1017/S1551929516000572.
[63] D. Bonen, S.L. Sarkar, The effects of simulated environmental attack on immobilization of heavy metals doped in cement-based materials, J. Hazard. Mater. 40 (3) (Mar. 1995) 321–335, https://doi.org/10.1016/0304-3894(94)00091-T.
[64] R.M. Santos, D.a. Ling, A. Sarvaramini, M. Guo, J. Elsen, F. Larachi, G. Beaudoin, B. Blanpain, T. Van Gerven, Stabilization of basic oxygen furnace slag by hot-stage carbonation treatment, Chem. Eng. J. 203 (2012) 239–250, https://doi.org/10.1016/j.cej.2012.06.155.
[65] A. van Zomeren, S.R. van der Laan, H.B.A. Kobesen, W.J.J. Huijgen, R.N.J. Comans, Changes in mineralogical and leaching properties of converter steel slag resulting from accelerated carbonation at low CO2 pressure, Waste Manag. 31 (11) (Nov. 2011) 2236–2244, https://doi.org/10.1016/J.WASMAN.2011.05.022.
[66] V. Caprai, K. Schollbach, H.J.H. Brouwers, Influence of hydrothermal treatment on the mechanical and environmental performances of mortars including MSWI bottom ash, Waste Manag. 78 (Aug. 2018) 639–648, https://doi.org/10.1016/j.wasman.2018.06.030.
[67] M. Bodor, R.M. Santos, G. Cristea, M. Salman, Ö. Cizer, R.I. Iacobescu, Y.W. Chiang, K. van Balen, M. Vlad, T. van Gerven, Laboratory investigation of carbonated BOF slag used as partial replacement of natural aggregate in cement mortars, Cem. Concr. Compos. 65 (2016) 55–66, https://doi.org/10.1016/j.cemconcomp.2015.10.002.